LAWRENCE
LIVERMORE
NATIONAL
LABORATORY

LLNL-JRNL-644651

Low Cloud Optical Depth Feedback in Climate Models

N. D. Gordon, S. A. Klein

October 10, 2013

Journal of Geophysical Research - Atmosphere

Low Cloud Optical Depth Feedback in Climate Models

Neil D. Gordon and Stephen A. Klein

Program for Climate Model Diagnosis and Intercomparison, Lawrence Livermore National Laboratory, Livermore, CA

Correspondence to: N. D. Gordon (gordon40@llnl.gov)

Abstract

The relationship between low-level cloud optical depth and atmospheric and surface air temperature is examined in the control climate of thirteen climate models to determine if cloud optical depth-temperature relationships found in observations are replicated in climate models, and if climate model behavior found in control climate simulations provides information about the optical depth feedback in climate warming simulations forced by increasing carbon dioxide. The regression of the natural logarithm of cloud optical depth with cloud temperature is strongly positive for all models for relatively cold clouds, while warmer clouds in the tropics and subtropics exhibit a negative relationship. This relationship is qualitatively similar to that in an earlier analysis of satellite observations, although models tend to have too positive a relationship for colder clouds and the inter-model spread is large. In the models, the cold cloud response comes from increases in cloud liquid and ice water content with increasing temperature, while in the tropics decreasing physical thickness *accompanies increasing cloud temperature. The intermodel and inter-regional spread of low-cloud optical depth feedback in climate warming simulations is well predicted by the corresponding spread in the relationships between optical depth and temperature for the current climate, suggesting that this aspect of cloud feedback may be constrained by present day observations. Because models have a positive bias relative to observations in the relationship between low-cloud optical and temperature, it is suggested that climate models simulate too great an increase in cloud optical depth at high latitudes leading to unrealistically large negative shortwave cloud feedbacks for climate changes.*

1. Introduction

The accurate simulation of cloud properties is a longstanding problem that inhibits confident projections of future climate. Previous research spanning several generations of climate models has shown that the intermodel spread in climate sensitivity is largely due to differences in cloud feedbacks (Cess et al., 1989, Soden and Held, 2006, DuFresne and Bony, 2008, Andrews et al. 2012, Vial et al., 2013). That small changes in clouds could alter climate sensitivity is suggested by the fact in the current climate, clouds, relative to clear-sky, reflect approximately 50 W/m^2 shortwave radiation and trap 30 W/m^2 more longwave radiation, globally averaged (Harrison et al., 1990), whereas the direct radiative impact of doubling carbon dioxide (CO_2) is only 3.7 W/m^2 (Myhre et al., 1998).

While cloud feedbacks can result from any change in cloud properties that significantly impacts the radiation budget of the planet, conceptually cloud feedbacks have been summarized as resulting from changes in three cloud properties: cloud amount, cloud altitude, and cloud optical depth (Schneider and Dickinson, 1974). In general, upon warming, climate models simulate decreases in cloud amount, particularly for low-level clouds at low-latitudes, and increases in cloud altitude, particularly for high clouds everywhere (Zelinka et al., 2012). Both the decreased reflection of shortwave radiation from the cloud amount decreases and the increased trapping of longwave radiation from the high cloud altitude increases contribute to the generally positive global mean cloud feedbacks exhibited by climate models. In contrast, climate models generally simulate increases in cloud optical depth with warming that tend to cause negative cloud feedbacks because the effects of increase cloud albedo on shortwave radiation overwhelm the impacts of increased cloud emissivity on longwave radiation. In some climate models from the 5th Coupled Model Intercomparison Project (CMIP5), negative shortwave cloud feedbacks from optical depth increases outweigh the positive shortwave cloud feedbacks from decreased cloud amount and lead to overall negative shortwave cloud feedbacks (Zelinka et al. 2013). This motivates research into the nature and causes of the optical depth feedback.

An important aspect of the optical depth feedback simulated by climate models is that it is non-uniform in space. Cold clouds, whether they are high-level clouds or lower-level clouds at high-latitudes, tend to become optically thicker with warming of the planet. In contrast, warm clouds, primarily low-level clouds at temperatures above about 0°C, tend to become optically thinner or exhibit little changes in optical depth with warming. The increased optical depth of clouds at high-latitudes is the main reason that nearly all climate models simulate negative shortwave cloud feedbacks at middle and high-latitudes. The contribution of the optical depth feedback to the latitudinal gradient in shortwave cloud feedbacks has caused speculation that optical depth feedbacks many influence the degree of polar amplification of the temperature warming exhibited in by climate models (Tselioiudis et al. 1993).

An intriguing aspect to the response of cloud optical depth to climate warming is the apparent similarity to the observed relationship between temperature and the optical depth of low-level clouds arising from natural climate variability on seasonal to interannual timescales. Specifically, both satellite (Tselioudis et al., 1992; hereafter T92) and in situ observations (Somerville and Remer, 1984) have found that the optical thickness of relatively cold low-level clouds increases with small increases of temperature, whereas satellite observations suggest that an opposite relationship exists for relatively warm low-level clouds (T92, Eitzen et al. 2011). This qualitative similarity between low-level cloud optical depth-temperature relationships in current climate observations and what climate models predict for low-level clouds for warmer worlds raises a very important question: Is the sensitivity of cloud optical depth to temperature on relatively short time scales predictive of the optical depth feedbacks that may occur on longer timescales? If so, it would allow us to use observations of clouds within our current climate to reduce inter-model spread in this feedback and potentially constrain the optical depth feedback for future climate change.

In this article, we analyze the behavior of low-cloud optical depth (hereafter τ_{low}) in an ensemble of climate models. We intend to (a) explore the degree of time-scale invariance to the relationship between τ_{low} and temperature, (b) document the ability of climate models to reproduce the observed relationships between τ_{low} and temperature, and (c) determine the relative contributions within models of changes in cloud physical properties to the relationship between τ_{low} and temperature.

The plan of the article is as follows. After a presentation of Methods (Section 2), we will examine the ability of models to replicate the observed relationships between τ_{low} and cloud temperature (Section 3). We will then examine the relative contribution of changes in water content and cloud physical thickness to the simulated relationships between τ_{low} and cloud temperature (Section 4). Following an examination of how τ_{low} relates to surface as opposed to cloud temperature in the current climate (Section 5), we will present how τ_{low} changes in climate model simulations of the climate change resulting from increases in CO_2 (Section 6). We then examine the correspondence between the relationship between τ_{low} and surface temperature in the current climate and that exhibited over climate changes (Section 7) before presenting our conclusions (Section 8).

2. Methods

We examine the climate models participating in the Cloud Feedback Model Intercomparison Project Phases 1 & 2 (CFMIP1, McAvaney and LeTreut, 2003; CFMIP2, Bony et al., 2011), projects aligned with phases 3 & 5 of CMIP, respectively. Of these models, we only use the thirteen models that provide the International Satellite Cloud Climatology Project (ISCCP, Rossow and Schiffer 1991, 1999) simulator output and atmospheric temperature (Table 1) at daily resolution in a control simulation (slabcntl in CFMIP1 and picontrol in CFMIP2) and a climate change scenario (2xCO2 in CFMIP1 and abrupt4xCO2 in CFMIP2) of atmospheric model coupled with a slab-ocean model for CFMIP1, and an interactive ocean for CFMIP2. For all but two CFMIP1 models (miroc_hi and miroc_lo – 2 years), there were five years of daily output for each of the two runs, while there were 20 years of simulation available for the CFMIP2 models. For the latter set of models, only the last 5 years of each model simulation were used to be consistent with the earlier models. The ISCCP simulator (Klein and Jakob, 1999, Webb et al., 2001) provides model cloud variables as if they were viewed by satellites used by ISCCP (Rossow and Schiffer, 1991, 1999), accounting for issues of cloud overlap and the assignment of cloud top pressure based upon an infrared brightness temperatures. This is an important tool for our study, as it is the only source of τ data in CFMIP and it allows us to understand how the τ behavior in climate models compare to that deduced from the analysis of ISCCP observations (T92). It also allows us to predict the extent to which cloud behavior that we can observe, via satellite platforms and within the current climate, can be extrapolated to future climates.

For each model, we take all time-space points with daily mean low-cloud (cloud-top pressure > 680 hPa) fraction greater than 10%, and less than 5% cloud fraction in all cloud layers above 680 hPa. The requirement for very small amounts of upper-level clouds is to better focus on low-level cloud scenes, although the results are similar if this restriction is eliminated (not shown). To determine a single value of cloud-top temperature for each point with low-level clouds, we calculate a cloud fraction weighted temperature using the model-predicted cloud fraction (i.e., not the ISCCP simulator determined cloud fractions) and temperature at each model layer below 680 hPa, assuming maximum cloud overlap for cloudy layers to determine the portion of clouds in each layer that are exposed to space. This allows us to simulate a cloud-top temperature of the low cloud as seen from a satellite, with perhaps a slight warm bias to the calculated temperature because the model temperature represent the mean of a layer, rather than the value at the top of a model level. Using the ISCCP simulator output, we derive a single value of τ_{low} for each grid-box with low-level clouds below 680 hPa by the amount of cloud present in the bin. We convert the mid-point of τ of each ISCCP simulator bin to reflectivity using an ISCCP look-up table, then calculate an average cloud reflectivity by weighting the reflectivity of each ISCCP histogram bin by the cloud fraction. The mean reflectivity is then converted to a mean τ_{low} using the same look-up table. This averaging technique ensures proper weighting based on amount of attenuated radiation.

Thus, for each valid observation as described above, we have a model-simulated cloud-top temperature and τ_{low}, and we will use an analysis technique similar to T92 to compute the relationship between these two variables. In this procedure, for each model, all observations are grouped by region based on latitude bands, and then are binned based on cloud temperature. From all data points falling within a given 15K wide bin of cloud temperature, a linear regression coefficient between the natural logarithm of τ_{low} and cloud-top temperature is calculated. The slope of this regression gives us the sensitivity of τ_{low} to temperature derived from variability at all time scales from daily through seasonal to interannual. Overlapping bins of cloud-top temperature are used to determine how the sensitivity of τ_{low} to temperature varies with the mean cloud temperature. Regressions slopes are not reported unless at least 50 grid-boxes are available with data and for which no fewer than 1/3 of the data points occur with temperatures on either side of the midpoint temperature for the bin.

It is also important to understand the source of changes in optical depth. In order to do so, it is helpful to recall the empirical relationship for liquid τ (Stephens 1978):

$$\tau = \frac{3}{2}\frac{q_l \delta z}{r_e} \quad [1]$$

where q_l is the average in-cloud liquid water content, assumed to be constant through the cloudy layers, δz is the cloud physical thickness in the vertical dimension, and r_e is the effective radius of cloud particles. While [1] does not apply directly for ice clouds, [1] remind us of the relevant variables we should attempt to examine. For the water content, we analyze the sum of in-cloud liquid and ice water contents and its relationship with temperature. All but three CFMIP1 models (hadgsm, hadsm3, and hadsm4) provide the grid-box mean cloud liquid and ice specific humidities on model layers (clw and cli, respectively). Volume-averaged in-cloud liquid plus ice water content is calculated using an estimate of cloud volume derived from the model-layer cloud fractions. Consistent with this, δz is calculated from the same vertical profile of cloud fraction assuming maximum overlap. Cloud particle size output is unavailable in the CFMIP archive. Attempts to infer its temperature derivative as a residual using [1] (not shown) suggest a small role for particle size variations consistent with scaling estimates provided in T92.

3. The relationship between low-cloud optical depth and cloud-top temperature in the current climate

Figure 1 shows the value of the linear regression coefficient of the natural logarithm of τ_{low} with cloud-top temperature (as described above) for clouds below 680 hPa. Figure 1a shows the results for land points, while Figure 1b shows the results for ocean points. Regression slopes are calculated separately for each of five regions, tropics (red - 0-15° latitude), subtropics (blue - 15-35°), midlatitudes (black - 35-55°), subpolar (green - 55-70°), and polar (magenta - 70-90°), using data from both the Northern and Southern Hemisphere. The value for each model is represented by a single symbol, while the solid line represents the multi-model median. The dashed lines in both figures reproduce the values derived from the ISCCP satellite observations by T92 which were calculated only for the tropical, subtropical and middle latitude regions over land and ocean separately.

We see some similarities and differences between the values calculated from observations and those calculated from the climate models. For the majority of models and regions, there is a common response of clouds colder than about 5°C, namely τ_{low} increases with increases in cloud-top temperature. But, for clouds warmer than 5°C, we see the opposite relationship, where τ_{low} decreases with increasing cloud-top temperature in the majority of models and regions. Some oceanic τ_{low} decreases with increases in cloud-top temperature are also present for temperatures colder than -25°C. Despite the similar shape and magnitude between the median of model results and those of T92, the multi-model median curves do not lie on top of those of T92, with the models tending to have a more positive value of the relationship between τ_{low} and cloud-top temperature than observed particularly for temperatures less than 5°C. Although the significance of which we are not sure, we note that in the medians, climate models reproduce the fact that the temperature derivative of τ_{low} is greater over land than ocean in the middle latitude regions with temperatures less than -10°C and subtropical regions with temperatures less than 0°C. The climate models we analyze here appear to be agree better with the observations in comparison to the GISS climate model analyzed in Tselioudis et al. (1993), which had comparable positive warm cloud feedbacks, but did not reproduce the robust cloud optical depth increases at cold temperatures.

We note that there is a wide diversity in cloud responses across the models. This is evident in range of feedback factor values that models display, even when the multi-model median is close to observations. For example, for midlatitude clouds over land (Fig. 1a) at -20°C, the multi-model median value temperature derivative of the logarithm of τ_{low} is 0.06 and the value derived from ISCCP observations by T92 is 0.05. But model values range from 0.02 to 0.21, spanning an order of magnitude. These intermodel differences are larger than the statistical uncertainties in the regression slope suggesting that real and significant inter-model differences exist.

While the uncertainty in the values of this parameter derived from the ISCCP observations are unclear, we have some evidence that inferences on model ability to simulate this parameter are robust to the choice of observational dataset. Using τ_{low} retrievals from the MODerate Resolution Imaging Spectrometer aboard the Aqua and Terra satellites, Eitzen et al. (2011) calculated the derivative between the logarithm of τ_{low} and sea surface temperature over subtropical regions known to have a large amount of stratocumulus, and found a value between -0.1 and -0.085, depending on the satellite platforms used. Using the same regions and comparing the model τ_{low} to surface air temperature instead of cloud-top temperature, we find a multi-model median value over all subtropical regions of 0.015, which is significantly more positive than the satellite results.

To test the robustness of the results to the methodology used for analysis, we also computed the relationship between the logarithm of τ_{low} and cloud-top temperature separately for each latitude and month of the simulations using all of the data from low-level cloud scenes at any longitude within a given month and latitude. For each month, the multi-model mean results demonstrate positive values at high-latitudes of each hemisphere and negative values at low-latitudes (not shown). This suggests that the simulated relationship between τ_{low} and cloud-top temperature shown does not depend on the inclusion of seasonal and interannual variability (which is included in the regression included in Figure 1). Furthermore, the latitude at which derivative transitions from negative to positive values moves poleward in the summer season of a given hemisphere roughly in-line with the movement of the 0°C isotherm of cloud-top temperature. This again suggests that the simulated relationship between τ_{low} and cloud-top temperature depends fundamentally on temperature and is not a function of the space or time-scale of the variability analyzed.

4. The role of cloud properties in low-cloud optical depth - temperature relationships in the current climate

In order to determine the relative importance of different cloud properties in contributing to the relationship between τ_{low} and cloud-top temperature, Figure 2 shows the regression slopes of all observations of the natural logarithms of (a) τ_{low}, (b) liquid plus ice water content, and (c) cloud physical thickness, all with respect to cloud-top temperature. Rather than display results for each latitude region and land and ocean separately as in Figure 1, we use a series of box and whisker plots for each cloud-top temperature of the regression slopes from all contributing regions regardless of whether the data was from land and ocean regions. The box and whisker plots show the minimum, 25th percentile, median, 75th percentile, and maximum regression slopes of each temperature bin.

Figure 2 suggests that the majority of the positive relationship between τ_{low} and cloud-top temperature at cold temperatures comes from an increase in cloud water content with temperature, while the negative relationship at warmer temperatures results from decreases in cloud physical thickness. While inter-model spread can be significant, these general characteristics are present in the majority of models individually.

With regard to cloud water content (Figure 2b), the temperature derivative of the logarithm of cloud water content is in magnitude similar to that reported by Somerville and Remer (1984) for liquid water content observed from in situ aircraft observations. Specifically, they reported a value of feedback factor of 0.04-0.05 across a temperature range between -25°C and +5°C. Over a similar range of temperature, the median model result is slightly larger, near 0.06 – 0.08. This may explain the propensity for models' to overestimate the relationship between τ_{low} and temperature at cold temperatures as compared to satellite observations (Figs. 1a and 1b).

As a physical explanation for this positive relationship between water content and temperature, it is tempting to invoke the temperature derivative to the adiabatic water content of clouds (Betts and Harshvardhan 1987). According to moist adiabatic theory, the adiabatic water content depends on the slope of the moist adiabat with respect to pressure. If the water content of clouds were a fixed fraction of the adiabatic water content, we would expect that the temperature derivative of logarithm of water content to be equal to the temperature derivative of the logarithm of the moist adiabat. The dashed line on Figure 2b shows the values of this derivative we calculate as a function of cloud-top temperature assuming a cloud-top pressure of 900 hPa. As shown by Betts and Harshvardhan (1987), this derivative is a strongly decreasing function of temperature with values near 0.07 per Kelvin at -25°C to values lower than 0.02 per Kelvin at temperatures above +10°C. The median model results also exhibit decreasing derivatives as the temperature rises but with larger values for temperatures in the range of -20°C to 0°C. Note that because the water content of clouds is a model-predicted variable subject to the influence of non-adiabatic processes such as mixing with the environment and precipitation, there is no guarantee that the water content of clouds would match that predicted solely from consideration of condensation processes along a moist adiabat.

Indeed, for temperatures beneath freezing it is possible that phase changes contribute to the positive derivatives of water content with temperature. Specifically, because of their characteristic sizes being larger leading to larger settling velocities, low-level stratiform clouds with ice-only tend to have a much lower water content than clouds that contain super-cooled water (Shupe et al.

2008). To the extent that temperature increases on average promote a reduction of the influences of ice, this phase transition would promote an increase of water content with temperature (Tsushima et al. 2006). The fact that particle sizes of ice tend to be larger than that of liquid also would contribute to an increase of τ_{low} with temperature.

With respect to cloud physical thickness, they tend to decrease with increases in cloud-top temperatures for warm clouds with little relationship or slight thickness increases for the coldest clouds (Figure 2c). Relative to water content, there is less inter-model spread that is difficult to explain although it may reflect that with poor vertical resolution there is little room of physical cloud thickness to vary systematically. The model result for the coldest clouds may be consistent with Lin et al. (2003) who found that in observations of Arctic low-clouds, cloud physical thickness tended to increase with warming by a lowering of cloud base and was the primary reason why liquid water paths increased at a rate of 0.03 K^{-1}.

Why models exhibit a negative relationship exists between cloud physical thickness and cloud-top temperature for warm temperatures is less well understood, although there are possible explanations from process-studies of subtropical marine boundary layer cloud. Bretherton and Wyant (1997) used a mixed-layer model of the stratocumulus-topped boundary layer to show that as boundary layer clouds were advected over warmer water, they tended to become more decoupled from the surface and the boundary layer deepened. This decoupling of the cloud layer from the surface reduced the moisture flux into the cloud, leading to a physically and optically thinner cloud. More recently, Large-Eddy Simulations of marine stratocumulus suggest physically thinner stratocumulus clouds would result with climate warming (under conditions of fixed-subsidence) (Blossey et al. 2013). Bretherton et al. (2013) interpret the LES cloud thinning with warming to result from the fact that a thinner cloud can sustain the same level of entrainment in the presence of a larger drop of absolute humidity between the surface and the free troposphere. However, it is unclear whether the climate models analyzed here have the physics necessary to simulate these mechanisms.

5. The relationship of low-cloud optical depth and properties to surface temperature in the current climate

We have related variations in τ_{low} and low-cloud properties to the cloud-top temperature in order to compare with the analysis based upon satellite observations which use cloud-top temperature (T92) as well as to document the relationship between low-level clouds and their actual temperatures. But, in order to relate current climate variability in low-level clouds to climate-change feedbacks, we need to document how low-cloud properties relate to variability in surface air temperature, the fundamental variable for climate feedback analysis. In Figure 3, we display the results of the analogous calculations to those in Figure 2 but using surface air temperature as the variable to which low-cloud properties have been regressed.

Apart from the expected shift in temperature resulting from the fact that temperatures at the surface are warmer than those in the cloud, the main features of the regression slopes remain largely the same. Specifically, we still see a positive relationship, between τ_{low} and the in-cloud values of water content and temperature for cold clouds, with values closer to zero at warm temperatures. An exception is that at warm temperatures, τ_{low} does not depend upon surface air temperature whereas a weak negative relationship was present in the relationship of τ_{low} to cloud-top temperature. This appears to result from the fact at these warm temperatures that the cloud physical thickness has a weak positive instead of negative relationship with temperature (Figure 3c). A positive relationship of cloud physical thickness with temperature would match the expectation that marine shallow convective clouds are taller with warmer surface air temperatures as shown by Large-Eddy Simulations (Rieck et al. 2012, Blosey et al. 2013), although it is unclear if this is the explanation for the model behavior.

6. The climate change response of low-cloud optical depth

We aim to examine the association of relationships between low-cloud properties and temperature arising from variability in the current climate with the response of low-clouds to carbon-dioxide induced warming. The simplest measure of the strength of the τ_{low} feedback in the climate change simulations is:

$$f_{actual} = \left[\frac{\Delta \ln\,(\tau_{low})}{\Delta T_{S,G}}\right] = \frac{\overline{\ln\left(\tau_{low,\uparrow CO_2}\right)} - \overline{\ln\,(\tau_{low,cntl})}}{T_{S,G,\uparrow CO_2} - T_{S,G,cntl}} \quad [2]$$

Calculated individually for each gridbox and model, this parameter is the difference in the mean τ_{low} between simulations with a climate change ($2xCO_2$ or $4xCO_2$) and the control integrations, divided by the change in global mean surface air temperature $T_{S,G}$. The overbar represents the time-mean average for a given gridbox, which for the CFMIP1 models is calculated as the means over the last 5 years of the 2 X CO_2 and control simulations – 30 years after the doubling of CO_2 was imposed. For CFMIP2 models, the means are calculated over the years 135-140 after CO_2 quadrupling and the corresponding years from the control simulation. Figure 4a shows the multi-model mean of this parameter which exhibits positive values near around +0.16 K^{-1} at high latitudes and near-zero values in the tropics or slightly negative values around -0.04 K^{-1} in subsidence regions over the low latitude oceans. Exceptions to this general behavior are found over Siberia and the Canadian Arctic. This pattern is generally similar to Figure 1 of Zelinka et al. (2012a), although it should be borne in mind that they show the τ change of all clouds, not just low clouds.

There is some intermodel spread to this pattern, particularly in the tropics which has fewer data points entering the calculation because our required conditions of a sufficient amount of low clouds without upper-level clouds present rarely occur. Although we require 5 observations per gridbox, in both the control climate and climate change simulations, in order to calculate this parameter, the paucity of observations and the fact that not every model may have enough observations to calculate a feedback parameter leads to spatial noise in the figure.

The changes in τ_{low} computed in this way may arise from changes in variety of factors such as thermodynamic environment of the clouds as well as changes in circulation. For a single model, we investigated the relative of these factors by computing changes in τ_{low} separately for different dynamical conditions. Specifically, for each grid box, we partitioned the daily-mean model output into quintiles based on both 500-mb vertical velocity and surface pressure. Both of these variables have been used for dynamical compositing of synoptic regimes (Norris and Weaver, 2000; Tselioudis et al., 2000). However, we found no difference in the calculation of τ_{low} feedback when compositing for dynamics using vertical motion and surface pressure as compared to the simple difference of grid box mean values between the 2xCO_2 and control climate integrations. This suggests a dominant role for thermodynamic conditions in explaining the climate changes in τ_{low}.

As noted in the introduction, an intriguing aspect of Figure 4a is the similarity of the climate change response to warming of τ_{low} with how τ_{low} varies with temperature in variability within the current climate. Specifically, positives values at high latitudes where the low-level clouds are cold and near zero or negative values at low-latitudes where low-level clouds are warm are at least superficially similar to the results in Figures 2a and 3a. Additionally, quantitatively the values shown in Figure 4a are similar in magnitude; this will be further tested in the next section. To display the similarity as a function of latitude and longitude, we have computed the regression of τ_{low} on local surface air temperature in each grid box and model from natural variability within the current climate. The multi-model mean of the local derivative of τ_{low} on local surface air temperature, shown in Figure 4b, again illustrates a great degree of similarity to the climate change response of τ_{low} in Figure 4a, with two noticeable differences. First, quantitatively the response in high-latitudes in Figure 4b is smaller than that in Figure 4a. We believe this results from the simple fact that in Figure 4a, we have normalized by the change in global mean surface air temperature. If we normalize by the local change in surface air temperature, which are larger than the global mean due to polar amplification of the warming (not shown), the values at high latitudes in Figure 4a would be smaller and in better agreement with those in Figure 4b. (This will quantitatively be tested in the next section). Second, in the deep tropics, there are some regions with positive regressions between τ_{low} and local surface air temperature. This appears to be significant even though the spatial noise is large due to the relative infrequency of low-level clouds. This may reflect the tendency of shallow convective clouds to grow in depth somewhat at the warmest temperatures (Figure 3c).

7. Timescale invariance of the relationship between low-cloud optical depth and surface temperature

Just as Hall and Qu (2006) demonstrated that the seasonal magnitude of the relationship between surface albedo and temperature is a good predictor of the snow-albedo feedback value for climate changes in climate models, we attempt to demonstrate whether such a relationship holds for the optical depth feedback of low-level clouds. We designed the following test which examines whether variations across model and latitudes in the relationship between τ_{low} and temperature are correlated across time-scale.

For each model and the 5 regions from the tropics to the poles, we calculate a mean value of the logarithmic derivative of τ_{low} on surface air temperature arising from variability within the current climate. This mean is calculated as a weighted average of the regression values that make up the curve in Figure 3a, where the weights are the number of low-level cloud instances used to calculated a regression at a given mean surface-air temperature in a given region and model. Using this average to represent the characteristic value for the region and model of the way that τ_{low} varies with surface air temperature, we then make a prediction of the climate change τ_{low} feedback by multiplying by the ratio of the change in surface air temperature averaged over the region to the change in global mean surface air temperature. This yields a predictive τ_{low} feedback factor f_{cntl}, based upon the relationship between τ_{low} and surface air temperature from the current climate:

$$f_{cntl} = \left[\frac{\sum_i \left(\frac{\partial \ln{(\tau_{low})}}{\partial T_{S,L}}_i * f_i\right)}{\sum_i f}\right]_{cntl} * \left(\frac{\Delta T_{S,R}}{\Delta T_{S,G}}\right)_{CO_2\uparrow - cntl} \quad [3]$$

In Equation 3, the first term is the weighted product of the feedback factor ($\delta\ln(\tau)/\delta T_{S,L}$) with respect to the local surface air temperature $T_{S,L}$ with the relative frequency of occurrence (f) of each surface air temperature bin, and the summation occurs over each of the 15K wide surface air temperature bins (i) for which τ_{low} was regressed on surface air temperature. The second term in Equation 3 is the average change in surface air temperature for a specific region ($\Delta T_{S,R}$) relative to the global-mean change in surface air temperature ($\Delta T_{S,G}$), both computed as a difference between the simulations with increased CO_2 and of the control climate. To obtain the analogous value for the actual τ_{low} feedback simulated by the model under climate change, we take the spatial average of the τ_{low} feedback from Eq. (2) over each region for each model that makes up the multi-model average plot of Figure 4a.

In Figure 5a, we display a scatterplot of the actual τ_{low} feedback from the climate change simulation on the y-axis and that predicted from the current climate on the x-axis for each of the 13 models and for each of the five regions. Each marker represents the average value for that model and a given region, and the colored line represents a least squares regression of the points which is performed separately for each of the 5 regions and then once again by combining the data from all of the regions (shown with a thick orange line). We have used the same colors and symbols as in Figure 1. The thin dashed line is a one-to-one line for reference, and would represent pure time scale invariance for the relationship of τ_{low} to temperature. For each region, there are positive relationships between the optical depth feedback predicted by a model's relationship between τ_{low} and temperature in the current climate, suitably scaled by the local to global temperature change after increased CO_2, to the climate change τ_{low} feedback actually simulated by the model. The value of r^2 for the regression that uses data from all regions is 0.61, and the midlatitude region having the most variance explained across models (0.72). From this evidence, we suggest that the relationship between τ_{low} and temperature does exhibit some degree of time-scale invariance but with two caveats. First, in a number or regions the regression slopes are biased such that the relationship between τ_{low} and temperature in the current climate over-predicts the magnitude of the τ_{low} feedback to climate change. Secondly, the lack of perfect correlation suggests that other factors besides thermodynamics influence the τ_{low} feedback, although the lack of perfect correlation could also result from errors in our methods used to measure and predict the τ_{low} feedback from the relationship between τ_{low} and temperature in the current climate.

Since much of the relationship between τ_{low} and temperature in current-climate variability arises from how the in-cloud water plus ice water content relates to temperature, we have also tested the time-scale invariance of water content in the exactly analogous way to that of τ_{low}. The result shown in Figure 5b shows very similar results to that of τ_{low}, suggesting that the way that the in-cloud water content of low-level clouds varies with temperature is the source of the time-scale invariance in τ_{low}.

8. Conclusions

We present our conclusions according to the 3 primary questions we seek to answer:

1) How well do climate models reproduce the observed relationships between τ_{low} and temperature?

In the ensemble mean, climate models appear to reproduce the observed characteristic that τ_{low} increases with temperature for cold low-level clouds, but decreases with temperature for warm low-level clouds. However, inter-model scatter is large and most models have a positive bias in the relationship of τ_{low} with temperature.

2) To what degree are the relationships between τ_{low} and temperature arising from natural variability within the current climate predictive of the response on longer-time scales of τ_{low} to warming induced by increases in CO_2?

Our tests indicate that inter-model and inter-region variability in the relationship between τ_{low} and temperature is to a large, but not complete, degree correlated across time-scale. This suggests that inter-model spread in the component of climate-change cloud feedbacks due to changes in τ_{low} can be reduced by improving the agreement between climate models and observations of the relationship between τ_{low} and temperature arising from natural variability from within the current climate. Furthermore, because models on average have a positive bias relative to the T92 observations in the relationship between τ_{low} and temperature, we suggest that the portion of high-latitude negative shortwave cloud feedbacks due to increases in τ_{low} may be too strong in models.

3) What are the relative contributions within models of changes in cloud physical properties to the relationship between τ_{low} and temperature?

Broadly speaking, the relationship of condensed water content inside the clouds to temperature are very similar to that of τ_{low} with temperature. Decreased physical cloud thickness with increases in temperature appear to partially contribute to the negative relationship between τ_{low} and temperature for warm low-level clouds.

Our work raises a number of important questions worthy of further study including:

1. What is the relative role of rapid adjustments (Gregory and Webb, 2008) to increases in CO_2 relative to temperature-mediated responses in explaining climate changes in τ_{low}? Zelinka et al. (2013) show that the τ feedback is actually stronger than previously thought once one removes the rapid reductions in τ that occur in response to increases in CO_2 but before warming occurs. Factoring in the rapid adjustments may partially explain why the τ_{low} feedback predicted from current climate variability overestimates the actual feedback simulated by the models (Figure 5). Unfortunately identical daily model output to that used in this study was not available to examine this question.

2. What are the physical processes that give rise to the model-simulated relationships with temperature of τ_{low} or water content? For cold clouds, is adiabatic theory really the reason that models on average simulate a rate of increase in water

content with temperature identical to that of the adiabatic water content? To what extent do phase changes contribute? For warm low-level clouds, what physical reasons explain why climate models on average simulate decreases in τ_{low} with temperature increases and why is the adiabatic lapse rate not a dominant factor?

3. Finally, what do newer and more complete observations inform us about the physical mechanisms that explain the relationship between temperature and τ_{low} or cloud properties? Many newer and more detailed satellite observations have been made available since the observational work of T92, and the active satellite sensors of CLOUDSAT (Stephens et al., 2002) and CALIPSO (Winker et al., 2009) would allow us explore the high latitude relationships that were not explored in T92 due to concerns of errors in retrievals over snow and ice. There is also the vast store of ground-based observations provided from sites maintained by the Atmospheric Research Measurement program (Ackerman and Stokes, 2004), which would allow for detailed in situ retrievals of cloud properties (such as cloud water content and physical thickness) at high time resolution. A study analyzing this ground-based data for the relationships of temperature with τ_{low} and low-level cloud properties is in preparation (Zhang et al. 2013).

Acknowledgments

The authors acknowledge the World Climate Research Program's Working Group on Coupled Modeling, which is responsible for CMIP, and we thank the climate modeling groups (listed in Tables 1 and 2 of this paper) for producing and making available their model output. For CMIP the U.S. Department of Energy's Program for Climate Model Diagnosis and Intercomparison provides coordinating support and led development of software infrastructure in partnership with the Global Organization for Earth System Science Portals. The authors acknowledge support by the Regional and Global Climate Modeling program of the United States Department of Energy's Office of Science, through a project entitled "Identifying Robust Cloud Feedbacks in Observations and Models". This work was performed under the auspices of the United States Department of Energy by Lawrence Livermore National Laboratory under contract DE-AC52-07NA27344.

References

Bony, S., and Coauthors, 2006: How Well Do We Understand and Evaluate Climate Change Feedback Processes? *J. Clim.*, **19**, 3445–3482.

Bony, S., M. Webb, C. Bretherton, S. Klein, P. Siebesma, G. Tselioudis, and M. Zhang (2011), CFMIP: Towards a better evaluation and understanding of clouds and cloud feedbacks in CMIP5 models, *CLIVAR Exchanges, 56*, International CLIVAR Project Office, Southampton, United Kingdom, 20-24.

Geophysical Fluid Dynamics Laboratory Global Atmosphere Model Development Team, 2004: The GFDL new global atmosphere and land model AM2/LM2: Evaluation with prescribed SST simulations. J. Climate, 17, 4641-4673.

Hall, A. and X. Qu (2006), Using the current seasonal cycle to constrain snow albedo feedback in future climate change, Geophys. Res. Lett., 33, L03502, doi:10.1029/2005GL025127.

Harrison, E. F., P. Minnis, B. R. Barkstrom, V. Ramanathan, R. D. Cess, and G. G. Gibson, 1990: Seasonal-variation of Cloud Radiative Forcing Derived from the Earth Radiation Budget Experiment. Journal of Geophysical Research-Atmospheres, 95, 18687-18703.

Hartmann, D.L., The Radiative Effect of Clouds on Climate. in *Aerosol-Cloud-Climate Interactions*, Ed. P.V. Hobbs, Academic Press, 151-170, 1993.

Johns, T. C., C. F. Durman, H. T. Banks, M. J. Roberts, A. J. McLaren, J. K. Ridley, C. A. Senior, K. D. Williams, A. Jones, G. J. Rickard, S. Cusack, W. J. Ingram, M. Crucifix, D. M. H. Sexton, M. M. Joshi, B-W. Dong, H. Spencer, R. S. R. Hill, J. M. Gregory, A.B. Keen, A. K. Pardaens, J. A. Lowe, A. Bodas-Salcedo, S. Stark, and Y. Searl, 2006: The new Hadley Centre climate model HadGEM1: Evaluation of coupled simulations, *Journal of Climate*, **19**, 1327-1353.

K-1 model developers, 2004: K-1 coupled model (MIROC) description, K-1 technical report, 1, H. Hasumi and S. Emori (eds.), Center for Climate System Research, University of Tokyo, 34pp.

Klein, S. A., and C. Jakob, 1999: Validation and sensitivities of frontal clouds simulated by the ECMWF model. *Monthly Weather Review*, **127**, 2514-2531.

Martin, G. M., Bellouin, N., Collins, W. J., Culverwell, I. D., Halloran, P. R., Hardiman, S. C., Hinton, T. J., Jones, C. D., McDonald, R. E., McLaren, A. J., O'Connor, F. M., Roberts, M. J., Rodriguez, J. M., Woodward, S., Best, M. J., Brooks, M. E., Brown, A. R., Butchart, N., Dearden, C., Derbyshire, S. H., Dharssi, I., Doutriaux-Boucher, M., Edwards, J. M., Falloon, P. D., Gedney, N., Gray, L. J., Hewitt, H. T., Hobson, M., Huddleston, M. R., Hughes, J., Ineson, S., Ingram, W. J., James, P. M., Johns, T. C., Johnson, C. E., Jones, A., Jones, C. P., Joshi, M. M., Keen, A. B., Liddicoat, S., Lock, A. P., Maidens, A. V., Manners, J. C., Milton, S. F., Rae, J. G. L., Ridley, J. K., Sellar, A., Senior, C. A., Totterdell, I. J., Verhoef, A., Vidale, P. L., and Wiltshire, A.: (2011) The HadGEM2 family of Met Office Unified Model climate configurations, Geosci. Model Dev., 4, 723-757, doi:10.5194/gmd-4-723-2011, 2011.

McFarlane, N.A., J. F. Scinocca, M. Lazare, R. Harvey, D. Verseghy, and J. Li, 2005: The CCCma Third generation atmospheric general circulation model. CCCma Internal Rep., 25 pp.

Myhre, G., E. J. Highwood, K. P. Shine, and F. Stordal, 1998: New estimates of radiative forcing due to well mixed greenhouse gases. *Geophysical Research Letters*, **25** (14), 2715-2718.

Norris, J. R., and C. P. Weaver, 2001: Improved techniques for evaluating GCM cloudiness applied to the NCAR CCM3. *Journal of Climate*, **14,** 2540-2550.

Pope, V., M.L. Gallani, P.R. Rowntree, R.A. Stratton, 2000, The impact of new physical parameterizations in the Hadley Centre climate model: HadAM3. Clim Dyn 16: 123-146.

Soden, Brian J., Isaac M. Held, 2006: An Assessment of Climate Feedbacks in Coupled Ocean–Atmosphere Models. *J. Clim*., 19, 3354– 3360. doi: 10.1175/JCLI3799.1

Somerville, R. C. J., and L. A. Remer, 1984: Cloud optical thickness feedbacks in the CO_2 climate problem. *J. Geophys. Res.*, 89, 9668-9672.

Stephens, G. L., 1978: Radiation profiles in extended water clouds. II: Parameterization Schemes. *Journal of the Atmospheric Sciences*, **35,** 2123-2132.

Stephens, Graeme L., and Coauthors, 2002: The CLOUDSAT mission and the A-Train. Bull. Amer. Meteor. Soc., 83, 1771–1790. doi: BAMS-83-12-1771

Stevens, B., Giorgetta, M. A., Esch, M., Mauritsen, T., Crueger, T., Rast, S., Salzmann, M., Schmidt, H., Bader, J., Block, K., Brokopf, R., Fast, I., Kinne, S., Kornblueh, L., Lohmann, U., Pincus, R., Reichler, T., & Roeckner, E., 2013: Atmospheric component of the MPI-M Earth System Model: ECHAM6. *Journal of Advances in Modeling Earth Systems*, 5, 146-172. doi:10.1002/jame.20015.

Tselioudis, G., W.B. Rossow, and D. Rind, 1992: Global Patterns of Cloud Optical Thickness Variation with Temperature. *J. Clim.*, 5, 1484– 1495.

Tselioudis, G., Y. C. Zhang, and W. B. Rossow, 2000: Cloud and radiation variations associated with northern midlatitude low and high sea level pressure regimes. Journal of Climate, 13, 312-327.

Watanabe, M., and Coauthors, 2010: Improved Climate Simulation by MIROC5: Mean States, Variability, and Climate Sensitivity. *J. Clim.*, 23, 6312–6335. doi: 2010JCLI3679.1

Watanabe, S., and Coauthors, 2011: MIROC-ESM 2010: model description and basic results of CMIP5-20c3m experiments. *Geosci. Model Dev.*, 4, 845–872.

Winker, David M., Mark A. Vaughan, Ali Omar, Yongxiang Hu, Kathleen A. Powell, Zhaoyan Liu, William H. Hunt, Stuart A. Young, 2009: Overview of the CALIPSO Mission and CALIOP Data Processing Algorithms. J. Atmos. Oceanic Technol., 26, 2310–2323. doi: 2009JTECHA1281.1

Yukimoto, S., Y. Adachi, M. Hosaka, T. Sakami, H. Yoshimura, M., Hirabara, T.-Y. Tanaka, E. Shindo, H. Tsujino, M. Deushi, R. Mizuta, S. Yabu, A. Obata, H. Nakano, T. Koshiro, T. Ose, A. Kitoh, 2012: A New Global Climate Model of the Meteorological Research Institute: MRI-CGCM3 —Model Description and Basic Performance, *J. Meteor. Soc. Japan*, 90A, 23-64.

Tables

Table 1 – List of models used in this study, their corresponding acronyms and citations.

Figures

Figure 1 – Regression of the natural logarithm of cloud optical thickness with cloud-top temperature for all observations grouped in 15°C-wide bins of cloud-top temperature, separately for each of five regions, tropics (red - 0-15°), subtropics (blue - 15-35°), midlatitudes (black - 35-55°), subpolar (green - 55-70°), and polar (magenta - 70-90°). Each model is represent by an individual dot, while the solid line represents the multi-model median value. The results of T92 are shown in black dashed lines. The analysis is done separately for (a) land points and (b) ocean points.

Figure 2 – Multi-model box and whisker plot of regression value with cloud top-top temperature for each model grid-box of the natural logarithm of (a) cloud optical depth, (b) cloud liquid water content, and (c) cloud physical thickness. The red line represents the median value, the interquartile range is spanned by the blue box, and the dashed lines extend to the minimum and maximum value for each temperature bin.

Figure 3 – Similar to Figure 2, but for regressions are calculated with respect to surface air temperature (TAS) for all regions together. The box and whiskers represent the minimum, 25^{th} percentile, median, 50^{th} percentile, and maximum of the feedback value among the 13 models at each temperature bin.

Figure 4 – (a) Multi-model mean climate change optical depth feedback parameter, calculated as the difference in natural logarithm of low cloud optical depth, divided by the difference in global mean surface temperature, both between the control and climate change integrations of all 13 CFMIP models. (b) Multi-model mean control climate regression value of the natural logarithm of optical depth and surface air temperature.

Figure 5 – Relationship between the optical depth feedback derived from the current climate (from Equation 3 - abscissa) and that for the climate change response (from Equation 2 - ordinate) for the tropics (red: 0-15°), subtropics (blue: 15-35°), midlatitudes (black: 35-55°), subpolar (green: 55-70°), and polar (magenta: 70-90°) regions. The colored lines represent a least-squares regression for each region, the orange dashed line is the least-squares regression for all regions together, and the thin dashed line is a one-to-one line for reference.

Table 1

	Model ID	Modeling Center	Reference
CMIP3/CFMIP1	CCCMA	Canadian Centre for Climate Modelling & Analysis	McFarlane et al. (2005)
	GFDL	US Dept. of Commerce / NOAA / Geophysical Fluid Dynamics Laboratory	Geophysical Fluid Dynamics Laboratory Global Atmosphere Model Development Team (2004)
	MIROC Hi	Center for Climate System Research (The University of Tokyo), National Institute for Environmental Studies, and Frontier Research Center for Global Change (JAMSTEC)	K-1 Model Developers (2004)
	MIROC Lo		
	HadGSM1	Hadley Centre for Climate Prediction and Research / Met Office	Johns et al. (2006)
	HadSM3		Pope et al. (2000)
	HadSM4		
CMIP5/CFMIP2	CanESM2	Canadian Centre for Climate Modelling & Analysis	McFarlane et al. (2005)
	HdGEM2-ES	Hadley Centre for Climate Prediction and Research / Met Office	Martin et al. (2011)
	MPI-ESM-LR	Max-Planck-Institut für Meteorologie (Max Planck Institute for Meteorology)	Stevens et al. (2012)
	MIROC-ESM	Japan Agency for Marine-Earth Science and Technology, Atmosphere and Ocean Research Institute (The University of Tokyo), and National Institute for Environmental Studies	Watanabe et al. (2010)
	MIROC5	Atmosphere and Ocean Research Institute (The University of Tokyo), National Institute for Environmental Studies, and Japan Agency for Marine-Earth Science and Technology	Watanabe et al. (2011)
	MRI-CGCM3	Meteorological Research Institute	Yukimoto et al. (2012)

Figure 1

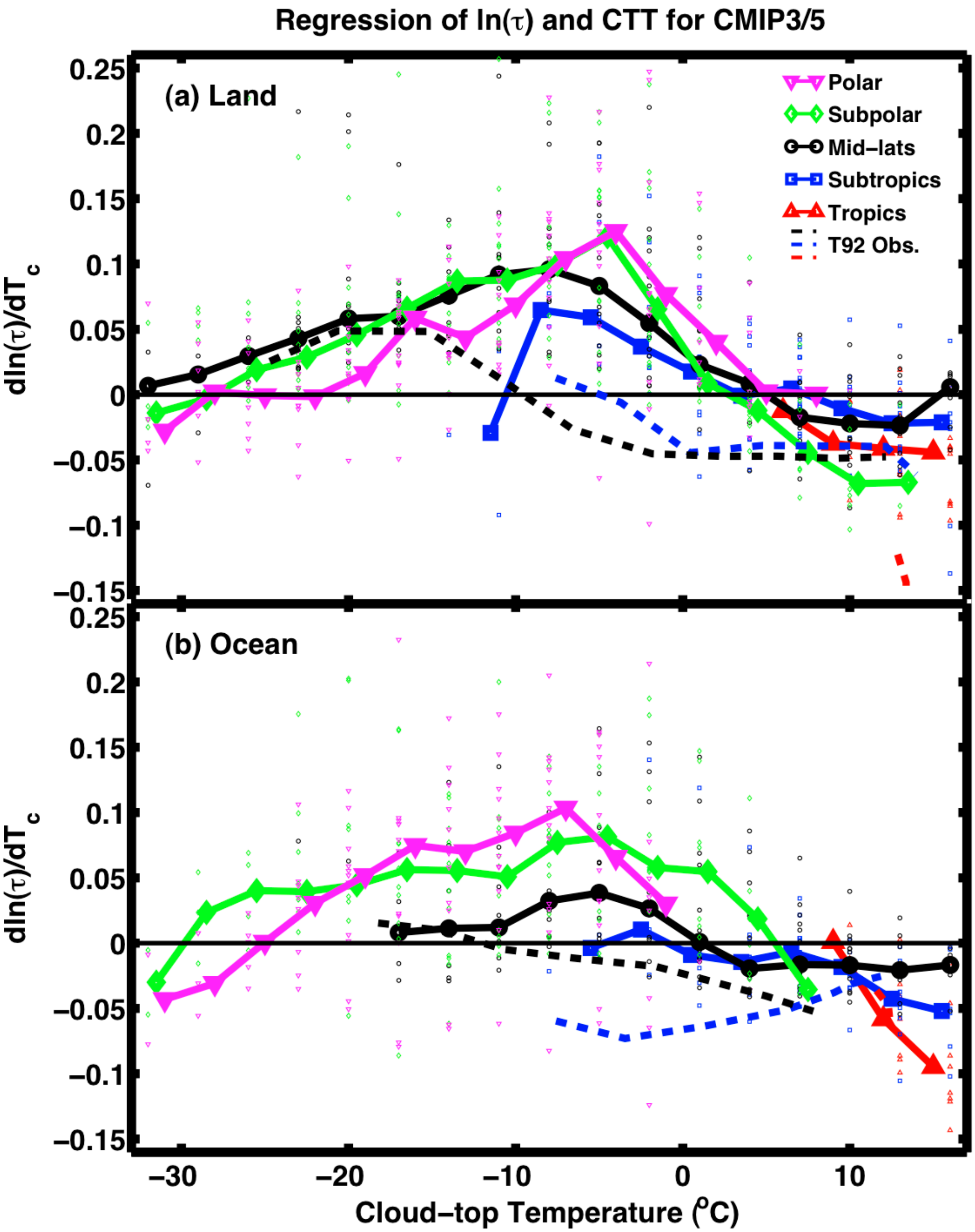
Regression of ln(τ) and CTT for CMIP3/5
(a) Land
(b) Ocean
Polar
Subpolar
Mid−lats
Subtropics
Tropics
T92 Obs.
dln(τ)/dT_c
0.25
0.2
0.15
0.1
0.05
0
−0.05
−0.1
−0.15
−30
−20
−10
0
10
Cloud−top Temperature (°C)

Figure 2

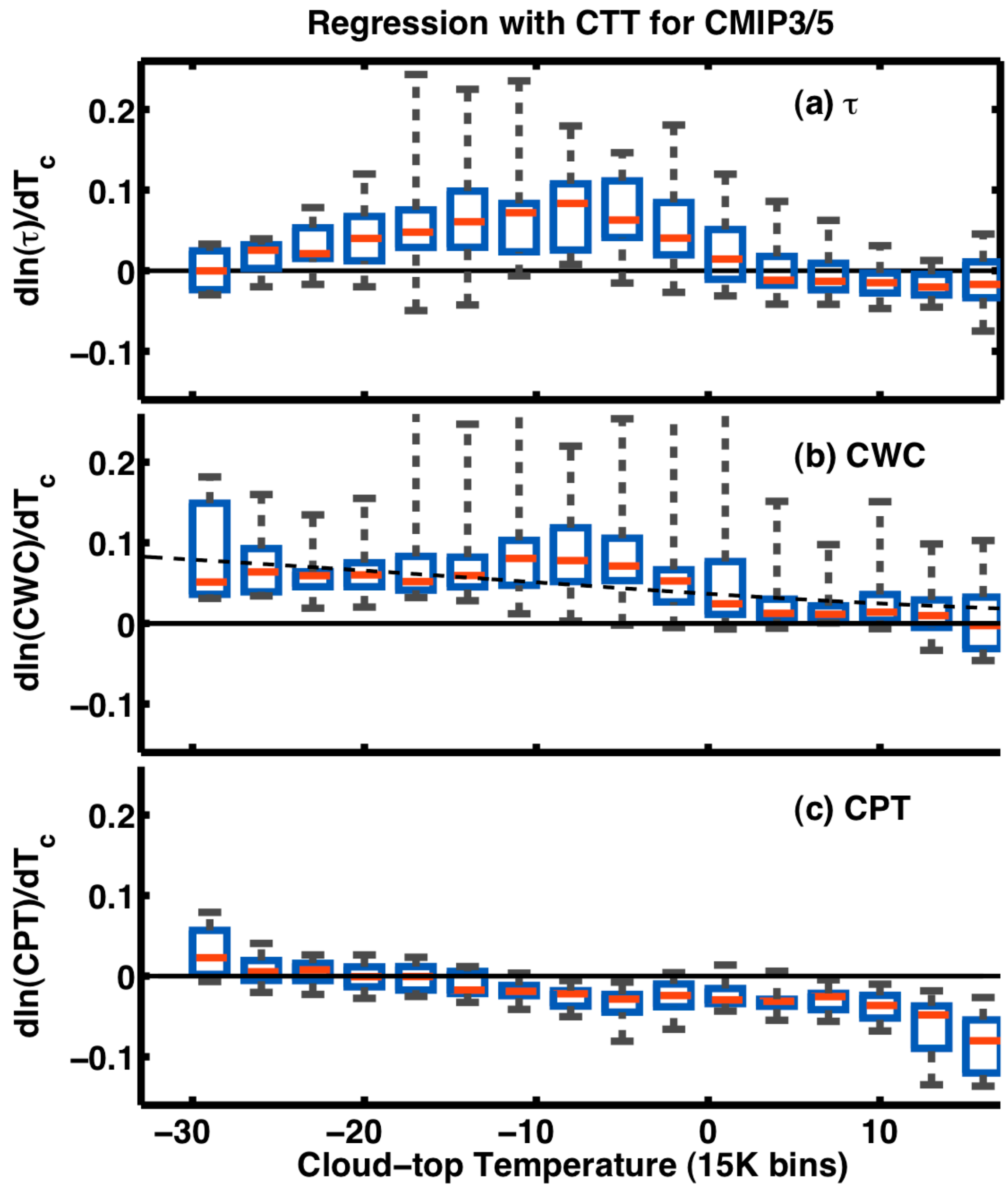

Regression with CTT for CMIP3/5
(a) τ
(b) CWC
(c) CPT
dln(τ)/dT c
dln(CWC)/dT c
dln(CPT)/dT c
0.2
0.1
0
−0.1
−30
−20
−10
0
10
Cloud−top Temperature (15K bins)

Figure 3

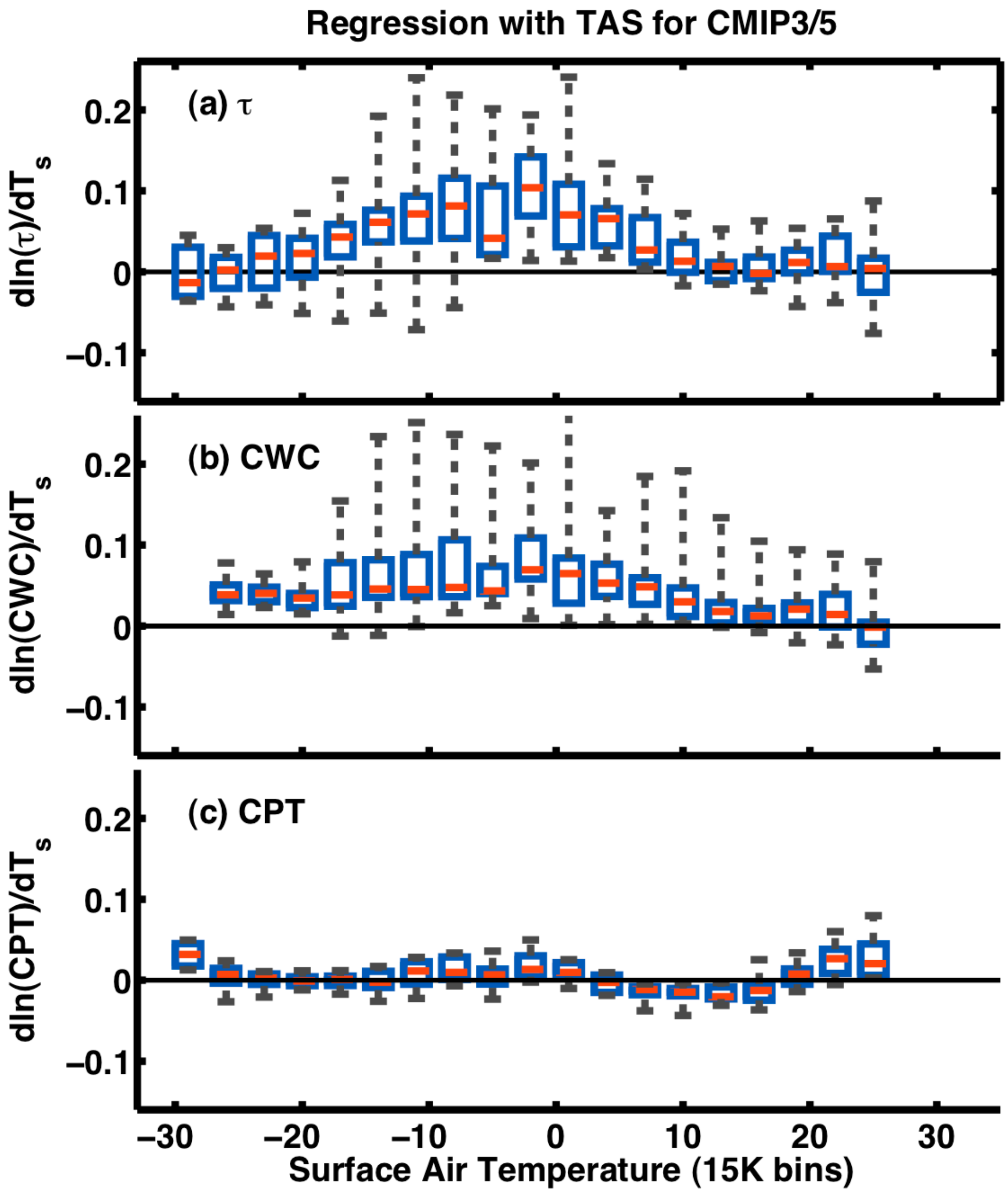

Regression with TAS for CMIP3/5
(a) τ
dln(τ)/dT s
(b) CWC
dln(CWC)/dT s
(c) CPT
dln(CPT)/dT s
0.2
0.1
0
−0.1
−30
−20
−10
0
10
20
30
Surface Air Temperature (15K bins)

Figure 4

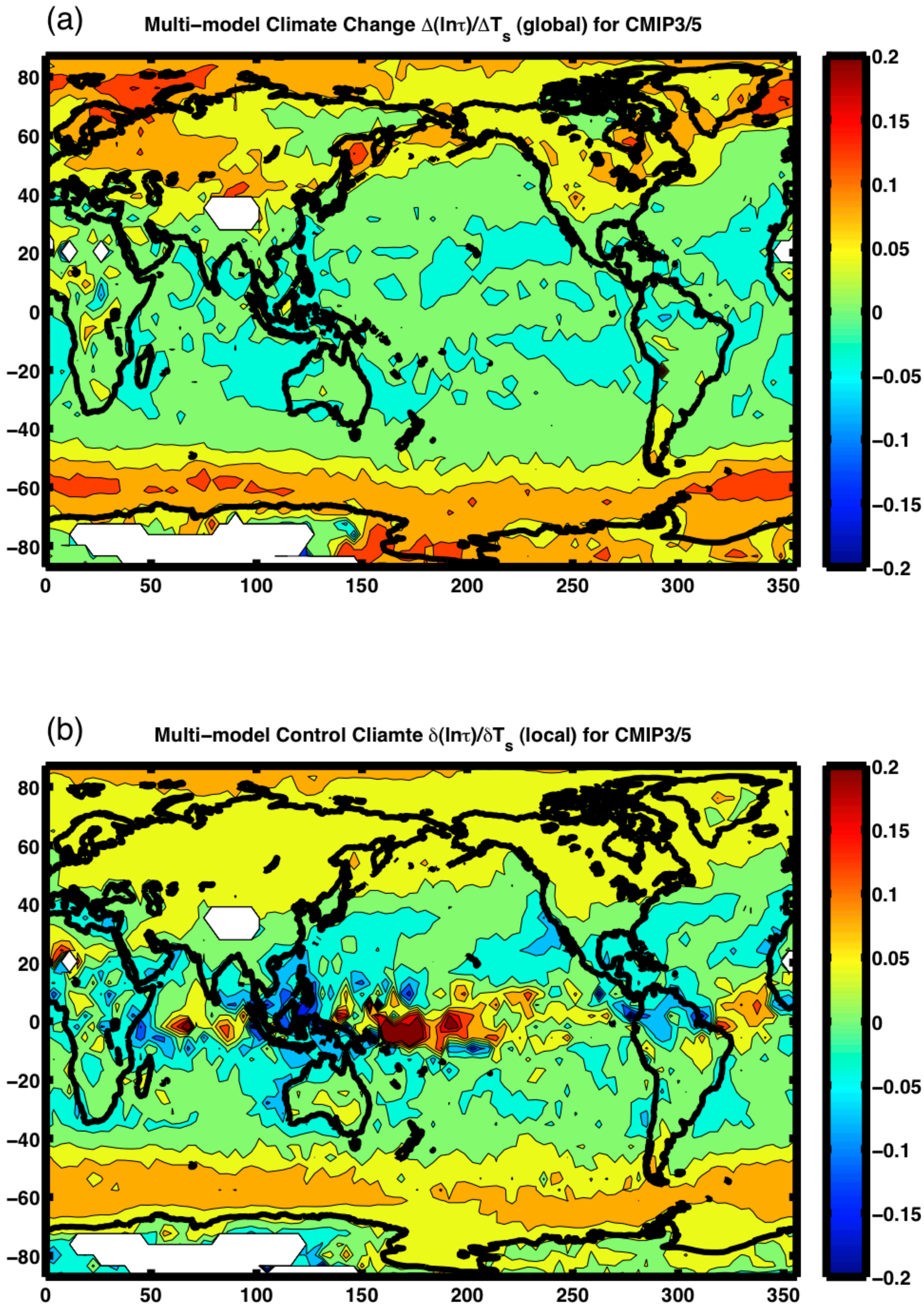
(a)
Multi–model Climate Change Δ(lnτ)/ΔT$_s$ (global) for CMIP3/5
80
60
40
20
0
−20
−40
−60
−80
0
50
100
150
200
250
300
350
0.2
0.15
0.1
0.05
0
−0.05
−0.1
−0.15
−0.2
(b)
Multi–model Control Cliamte δ(lnτ)/δT$_s$ (local) for CMIP3/5
80
60
40
20
0
−20
−40
−60
−80
0
50
100
150
200
250
300
350
0.2
0.15
0.1
0.05
0
−0.05
−0.1
−0.15
−0.2

763 Figure 5

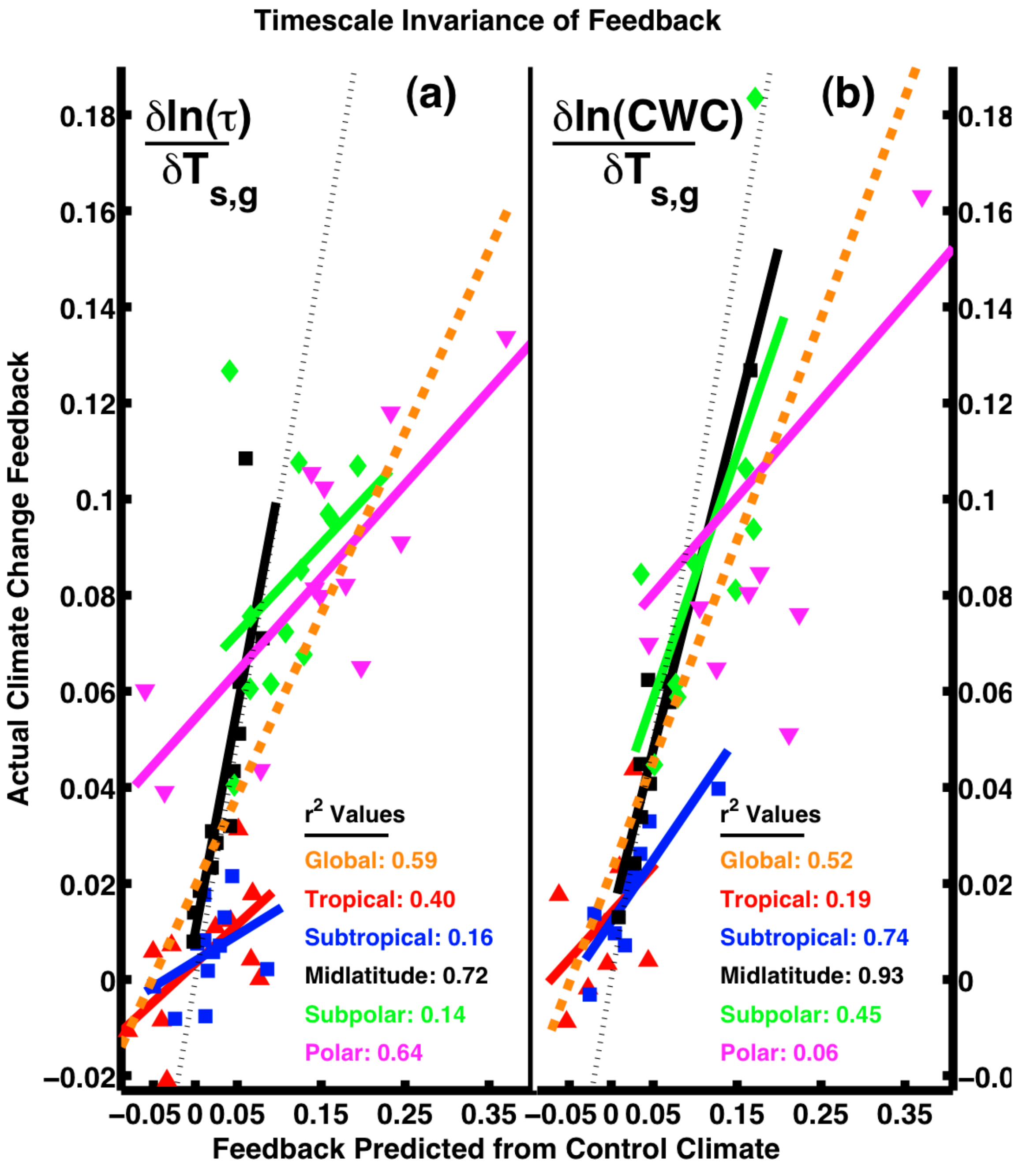

764